Statistical Analysis of the Multiple Scattering Radio Channel

Jari Salo, Hassan M. El-Sallabi and Pertti Vainikainen

Abstract

The concept of multiple scattering radio propagation channels – in contrast to the conventional single (Rayleigh) scattering – has been proposed and found to be a fitting model in certain propagation scenarios. Except for some special cases, expressions for the amplitude distribution of such channels are unknown. In this paper we derive distribution functions for the amplitude of the general multiple scattering radio channel. Rice, Rayleigh and double-Rayleigh distributions are special cases of the general result. We also derive a computationally simple moment-based estimator for the parameters of the distribution. In addition to the measurement analysis of multiple scattering propagation channels, our results can also be applied in the performance evaluation of communication schemes over such media.

I. Introduction

The Rayleigh distribution is the classical amplitude fading distribution of wireless communications channels. It has stood the test of time due to its simplicity, and has been experimentally shown to be a good probability model for received signal envelope in a wide variety of propagation conditions [1]. From a physical modelling point of view, the Rayleigh distribution is well justified, as the received signal can be assumed to be a superposition of a large number of randomly phased waves. It then follows from the central limit theorem that the real and imaginary parts of their sum have approximately Gaussian distribution, which, in turn, leads to Rayleigh-distributed magnitude. Numerous generalizations of the Rayleigh distribution have been

The authors are with SMARAD CoE, Radio Laboratory, Helsinki University of Technology, P.O. Box 3000, FI-02015 TKK, Finland (e-mail: jari.salo@tkk.fi, hsallabi@cc.hut.fi, pertti.vainikainen@tkk.fi). The work has been supported by the Academy of Finland, Foundation of Commercial and Technical Sciences, Nokia foundation, TKK foundation, and Graduate School of Electronics, Telecommunications, and Automation (GETA).

suggested, including the Rice, Nakagami-m, and Suzuki distributions [2]. All these distributions are well motivated physically and include the Rayleigh probability model as a special case.

Recently, yet another generalization, the so-called multiple scattering model, has been proposed [3], [4]. To explain the idea, we first consider the special case of double scattering, shown in Fig. 1a, where the transmitted signal can propagate to the receiver only through an electromagnetically small aperture, a keyhole. If the transmitter is moving, the signal envelope at the keyhole will have Rayleigh fading amplitude due to summation of multiple plane waves, say, $h_{tx} = \sum_k a_k e^{j\theta_k}$ for a given time instant. Assuming that the receiver is also moving, each wave propagating though the keyhole, $a_k e^{j\theta_k}$, will multiply another, independent sum of plane waves, $h_{rx} = \sum_k b_k e^{j\phi_k}$. If the number of scatterers on both sides of the screen is large, the envelope of the resulting narrow-band impulse response, $h = h_{tx}h_{rx}$, will have the double-Rayleigh distribution [5] when sampled over time. (In this simple example we have assumed that the transmitter, the keyhole, and the receiver all operate on the same polarization.)

The notion of keyhole, introduced in [6], is only a conceptual aid, whose role is in reality played by some more worldly item. Examples of real-world keyholes are shown in Fig. 2.

- *Fig. 2a:* When two rings of scatterers are separated by a large distance ($r \ll R$), all propagation paths travel via the same narrow "keyhole" [3], [7].
- *Fig. 2b:* Propagation in amplify-and-forward wireless relay networks. An amplify-and-forward node is essentially a keyhole. Here we assume that the analogue repeater node (A-F) has fixed gain, which will result in double-Rayleigh signal amplitude (however, noise of the A-F node will affect receiver noise and hence bit error analysis [8]). The wireless peer-to-peer concept has recently received a great deal of attention in the communications community [9]. Amplify-and-forward is one example of a relay functionality that have been proposed to be used in relay networks [8] [10].
- *Fig. 2c:* Propagation via diffracting wedges, such as street corners or rooftops. The street corner essentially functions as a multiplier for the two Rayleigh processes [11].

It should be noted that in multiple-input multiple-output (MIMO) channels the existence of a keyhole in the signal path will, in principle, cause rank reduction in the channel matrix [6], [7]. It is currently a much debated question in radio propagation research community whether keyholes exist. Intuition and results from controlled laboratory experiments [12] suggest that pure keyholes – even if they exist – are difficult to find due to practical measurement problems.

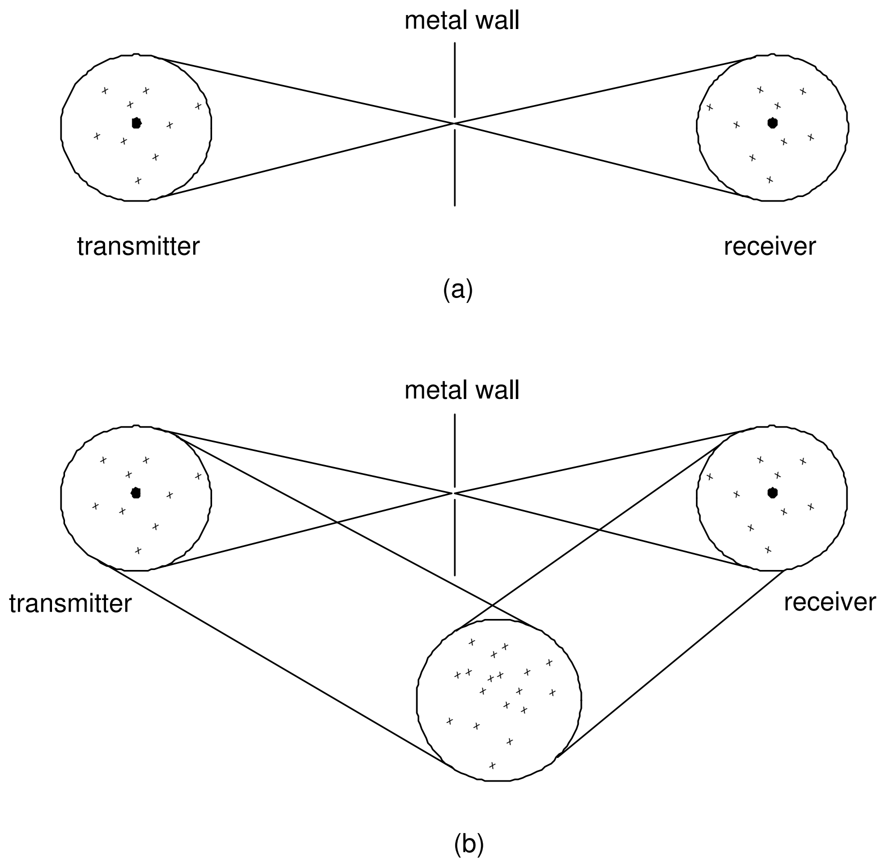

Fig. 1. Conceptual explanation of: (a) double scattering propagation; (b) mixture of single and double scattering due to unideal keyhole (“leaky keyhole” channel).

Therefore it is reasonable to turn attention to more realistic models, that might better explain the apparent rare occurrence of keyholes and double-Rayleigh amplitude in measurements.

In a real world propagation scenario it is a somewhat unrealistic assumption that the received signal would be a result of a pure double scattering process shown in Fig. 1a. It is more probable that the transmitted signal undergoes a combination of single and double scattering, shown in Fig. 1b, where the single scattering (Rayleigh amplitude) signal bypasses the keyhole [13]; we call this the “leaky keyhole” channel, for short. More generally, the model can be generalized to include multiple scatterers and line-of-sight component as proposed in [3], [4]. The general multiple scattering model therein yields as special cases Rice, Rayleigh and double-Rayleigh channels, arguably making it the most general physically motivated propagation model proposed so far.

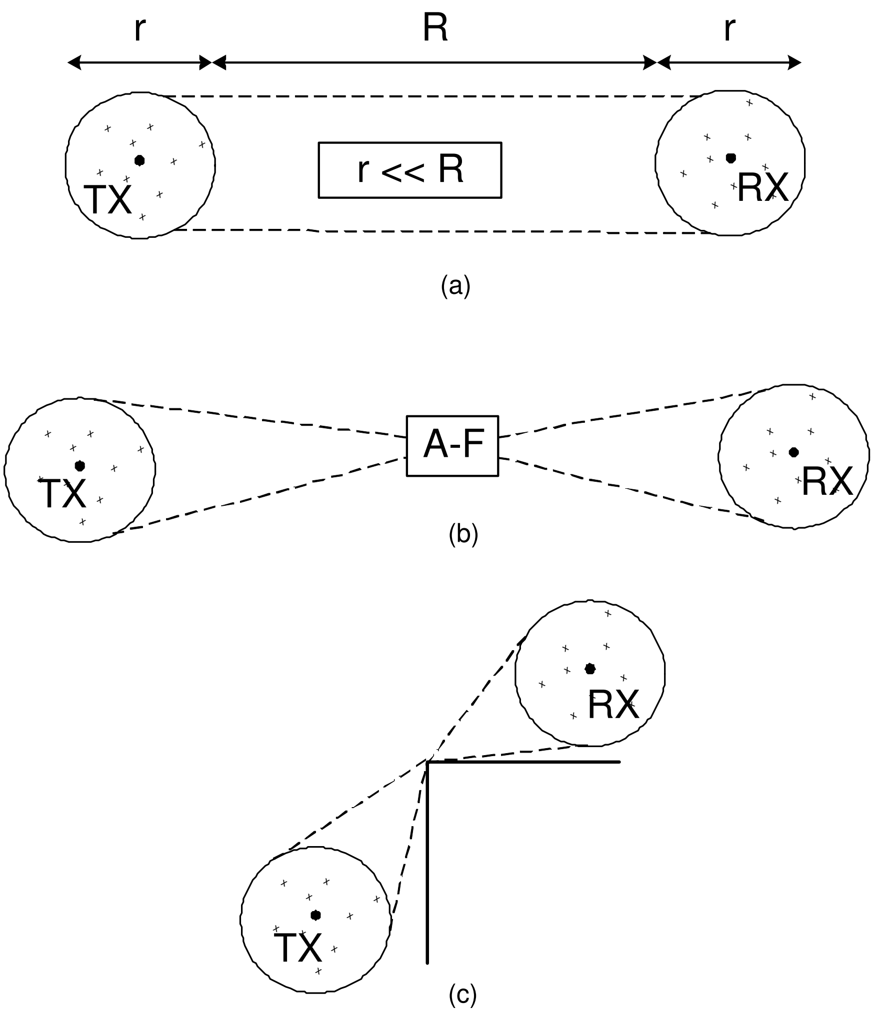

Fig. 2. Three propagation scenarios with a keyhole: (a) keyhole created by two rings of scatterers separated by large distance [7]; (b) amplify-and-forward relay; (c) propagation via diffracting street corner [11].

The number of available experimental studies of the multiple scattering channel is limited. It has been found to provide a good explanation for the signal envelope in certain types of radio channels, both in simulation [11] and measurements in urban, suburban and forest environments [3], [4], [14], [15]. In order to facilitate further studies, it is important to derive analytical tools and as well as to try to understand its fundamental physical and statistical characteristics. Certain properties of the multiple scattering process – to be discussed later in the paper – make its measurement and data analysis somewhat difficult.

In this paper, instead of embarking on a channel measurement tour, we execute an analytical flank attack on the topic, and focus on the statistical characterization of the multiple scattering channel model. As our main contribution we derive the amplitude distribution functions of the generalized multiple scattering radio channel. To the best of our knowledge, these distributions have been unknown, and consequently Monte Carlo simulations have been used in earlier studies. We also supply a computationally simple moment-based estimator for the parameters of the multiple scattering amplitude distribution. The analytical results in this paper can be used in processing of radio channel measurement data, evaluation of the error performance of communication schemes, computation of SNR outage probabilities etc.. The results generalize our earlier work reported in [16], [17].

The paper is organized as follows. In Section II we present the multiple scattering signal model. In Section III the distribution functions are derived for the amplitude of the general multiple scattering signal, whereas in Section IV we focus on the special case of second-order scattering. Section V discusses moment-based estimator of the distribution parameters. Some numerical examples are presented in Section VI. Section VII concludes the paper. Throughout the paper we shall use various special functions, whose notation and definitions are summarized in Table I. For alternative definitions and further details on the special functions, we refer to standard references, e.g. [18]–[20].

Remark on terminology: As in [3], [4], by multiple scattering we mean a radio signal that can be described as a linear combination of signal components with constant, Rayleigh, double-Rayleigh etc distributed amplitude; the mathematical signal model will be defined in Equations (1)–(4). In radio channel modelling the terms single and double scattering are sometimes also used to refer to single-*bounce* and double-*bounce* interactions, especially in the context of geometric channel models. However, it should be noted that a multiple-bounce signal does not in general have multiple-Rayleigh amplitude distribution as this requires the existence of a keyhole in the signal path (but see Fig. 2a).

II. Signal model

We model a realization of the narrow-band impulse response of the multiple scattering radio channel as [3], [4]

TABLE I

NOTATION AND DEFINITIONS

Name	Notation[a]	Definition
Upper incomplete gamma	$\Gamma_{\mathrm{u}}(a,x)$	$\int_x^\infty t^{a-1}e^{-t}\ \mathrm{d}t$
Lower incomplete gamma	$\Gamma_{\mathrm{l}}(a,x)$	$\int_0^x t^{a-1}e^{-t}\ \mathrm{d}t$
Gamma	$\Gamma(a)$	$\Gamma_{\mathrm{u}}(a,0)=\Gamma_{\mathrm{l}}(a,\infty)$
Pochhammer symbol	$(a)_k$	$\prod_{m=1}^k (a+m-1)$, $(a)_0=1$
Exponential integral	$\mathrm{E}_\nu(x)$	$\int_x^\infty t^{-\nu}\, e^{-t}\ \mathrm{d}t$
Bessel function (1st kind)	$J_\nu(x)$	$\pi^{-1}\int_0^\pi \cos(\nu\theta - x\sin\theta)\,\mathrm{d}\theta$
Meijer G-function	$G_{p,q}^{m,n}\left(x\middle\vert\begin{smallmatrix}\{a_k\}\\ \{b_k\}\end{smallmatrix}\right)$	$\frac{1}{j2\pi}\int_{\mathcal{L}}\frac{\prod_{k=1}^m\Gamma(b_k+s)\prod_{k=1}^n\Gamma(1-a_k-s)\,x^{-s}}{\prod_{k=n+1}^p\Gamma(a_k+s)\prod_{k=m+1}^q\Gamma(1-b_k-s)}\,\mathrm{d}s$
Hypergeometric function	${}_2F_1(a,b;c;x)$	$\sum_{k=0}^\infty \frac{(a)_k(b)_k}{(c)_k}\frac{x^k}{k!}$
Laguerre polynomial	$L_m(x)$	$\sum_{k=0}^m (-1)^k\binom{m}{k}\frac{x^k}{k!}$
Expected value	$\mathrm{E}[X]$	Expected value of X
kth moment	$\mu_X^{(k)}$	$\mathrm{E}[X^k]$, $\mu_X^{(1)}=\mu_X$
Variance	$\mathrm{var}[X]$	$\mathrm{var}[X]=\mu_X^{(2)}-(\mu_X)^2=\mu_X^{(2)}-\mu_X^2$

[a] ν, m, n, p, q and k are non-negative integers. $\mathcal{L}$ is an integration contour that depends on the parameters of the Meijer G-function [19].

$$\begin{aligned} C_N^\star &= w_0 e^{j\theta} + w_1 H_1 + w_2 H_2 H_3 + \text{up to } (N+1)\text{th summand} \\ &= \sum_{n=0}^N C_n\,, \end{aligned} \tag{1}$$

where $C_0 = w_0 e^{j\theta}$ is the line-of-sight component with constant magnitude w_0 and uniformly distributed phase θ over $[0, 2\pi)$, and

$$C_n = w_n \prod_{i\in I(n)} H_i\,, \quad n>0\,, \tag{2}$$

where $I(n) = \{\frac{n(n-1)}{2}+j\}_{j=1}^n$ is the index set, and H_i's are independent, identically distributed (iid) isotropic zero-mean Gaussian random variables[1] such that $\mathrm{E}[|H_i|^2]=1$. It follows that $C_N^\star$ is an isotropic random variable with $\mathrm{E}[|C_N^\star|^2]=\sum_{n=0}^N w_n^2$. The weights $\{w_n\}_{n=0}^N$ are non-negative

[1]Let $Z = X + jY$ be a complex random variable. If Z and $Ze^{j\theta}$ have the same distribution for arbitrary real θ, then Z is called an isotropic random variable. If X and Y are iid Gaussian, then Z is called an isotropic Gaussian random variable, or, equivalently, circularly symmetric complex Gaussian random variable.

real-valued constants that determine the mixture weights of the multiple scattering components. We call the integer N in (1) the scattering order, and the underlying physical process Nth order multiple scattering. For example, third-order scattering ($N = 3$) results in

$$C_3^\star = w_0 e^{j\theta} + w_1 H_1 + w_2 H_2 H_3 + w_3 H_4 H_5 H_6 \,.$$

Conventionally, only the first-order scattering is assumed, i.e., $w_n = 0$, for all $n > 1$; this results in the conventional Rician fading signal magnitude (or Rayleigh, if $w_0 = 0$).

We adopt the following notation:

$$R_N^\star = |C_N^\star| \tag{3}$$

$$R_n = |C_n| \,. \tag{4}$$

The '$\star$' notation in (3) indicates summation of the first N multiple scattering components and the constant-magnitude component, while R_n is an 'n-Rayleigh' random variable defined as the product of n independent Rayleigh random variables. The double-Rayleigh distribution has been derived in e.g. [5], [14], [21]. The distribution of R_n for arbitrary n is a special case of the general result in [22], and was recently independently re-derived in [17]. Other closely related special cases of [22] include the products of independent Nakagami-m [23] and generalized gamma variables [24].

III. Distribution functions of $R_N^\star$

In this section we shall derive the probability density and distribution functions of $R_N^\star = |C_N^\star|$ for the general Nth order scattering model in (1). Both integral and series forms are provided.

A. Distribution functions in integral form

We first introduce some notation. The characteristic function of a complex-valued random variable $Z = X + jY$ with uniform phase over $[0, 2\pi)$ is denoted $\Phi_Z(\omega)$, where $\omega = \sqrt{\omega_X^2 + \omega_Y^2}$ and $X \leftrightarrow \omega_X$ and $Y \leftrightarrow \omega_Y$ are variable pairs in the Fourier transform relationship between probability densities and characteristic functions. Due to uniformly distributed phase of Z, the integral kernel in the two-dimensional Fourier transform is radially symmetric, which allows us to write the characteristic function of two real variables using only a single "radius" parameter ω. It follows that the pdf of $|Z|$ and $\Phi_Z(\omega)$ are related by a Hankel transform [25]. To be more precise, the scalar variable function $\Phi_Z(\omega)$ should be called the characteristic generator [26]. We shall, however, slightly misuse the terminology and throughput the paper refer to $\Phi_Z(\omega)$ as the characteristic function of a circular random variable Z.

Since $C_N^\star$ is isotropic, its phase is uniformly distributed over $[0, 2\pi)$ and independent of $R_N^\star$. The pdf of $R_N^\star$ is given by the inverse Hankel transform [25]

$$f_{R_N^\star}(r) = r \int_0^\infty \omega \, \Phi_{C_N^\star}(\omega) J_0(r\omega) \, \mathrm{d}\omega \,, \tag{5}$$

where $\Phi_{C_N^\star}$ is the radially symmetric characteristic function of the complex random variable $C_N^\star$, and $J_0(x)$ is the Bessel function of the first kind. The same general technique has been applied earlier for deriving the distribution of a sum of random sinusoids with and without Gaussian noise [27], [28].

Due to independence of C_n's the characteristic function of $C_N^\star$ in (1) is the product of the characteristic functions of the summands:

$$\Phi_{C_N^\star}(\omega) = \prod_{n=0}^{N} \Phi_{C_n}(\omega) \,. \tag{6}$$

In order to compute the general integral form of the density function (5) it remains to find an expression for $\Phi_{C_n}(\omega)$. Based on the inverse relationship of (5) the characteristic function of any circularly symmetric complex random variable can be found as the Hankel transform of its amplitude distribution function, and therefore

$$\Phi_{C_n}(\omega) \;\; = \;\; \int_0^\infty f_{R_n}(r) \, J_0(\omega \, r) \, \mathrm{d}r \,. \tag{7}$$

For the line-of-sight component $f_{R_0}(r) = \delta(r - w_0)$, leading to

$$\Phi_{C_0}(\omega) = J_0(w_0\omega) \,. \tag{8}$$

For general $n > 0$, it turns out, the characteristic function can be stated in terms of generalized hypergeometric functions. The density of the n-Rayleigh random variable is [17]

$$f_{R_n}(r) = \frac{2}{w_n} G^{n,0}_{0,n}\left(\left(\frac{r}{w_n}\right)^2 \Big|^{-}_{\{\frac{1}{2}\}_n} \right) , \tag{9}$$

where $G^{m,n}_{p,q}(\cdot)$ is the Meijer G-function [19], and we denoted

$$\{a\}_n = \{\underbrace{a, \ldots, a}_{n \text{ times}}\} .$$

Inserting (9) to (7) we obtain from the Meijer G-function identity [20, §07.34.21.0091.01]

$$\Phi_{C_n}(\omega) = \frac{2}{w_n \omega} G^{n-1,1}_{1,n-1}\left(\left(\frac{2}{w_n \omega}\right)^2 \Big|^{\frac{1}{2}}_{\{\frac{1}{2}\}_{n-1}} \right) , \tag{10}$$

which is the characteristic function of an n-Rayleigh distribution for arbitrary $n > 0$. From (5) and (6), it follows that the probability density function of the amplitude for Nth order multiple scattering case is

$$f_{R^\star_N}(r) = r \int_0^\infty \omega \prod_{n=0}^{N} \Phi_{C_n}(\omega) J_0(r\omega) \, \mathrm{d}\omega , \tag{11}$$

where $\Phi_{C_n}(\omega)$, for $n = 0$ and $n > 0$ are given in (8) and (10), respectively.

Although the Meijer G-function has been implemented in many mathematical software packages, the integral (11) is in general computationally expensive to evaluate numerically. To alleviate the problem, for $n < 4$ the characteristic function can be expressed in terms of less general functions using various Meijer G-function identities available in literature [20], [29], [30]. In particular, we have

$$\begin{aligned}
\Phi_{C_1}(\omega) &= \exp\left(-\frac{w_1^2 \omega^2}{4}\right) , & (12)\\
\Phi_{C_2}(\omega) &= \frac{4}{4 + w_2^2 \omega^2} , & (13)\\
\Phi_{C_3}(\omega) &= \left(\frac{2}{w_3 \omega}\right)^2 e^{(\frac{2}{w_3 \omega})^2} \, \mathrm{E}_1\left((\frac{2}{w_3 \omega})^2 \right) , & (14)
\end{aligned}$$

where $\mathrm{E}_1(x)$ is the exponential integral defined in Table I. The case $n = 1$ is the characteristic function of an isotropic complex Gaussian random variable, and hence well-known from literature [28]. Interestingly, $\Phi_{C_2}(\omega)$ is the characteristic function of the Laplace distribution, which implies that the real and imaginary parts of double-Rayleigh fading channel are Laplace distributed; this has been noted also in [10].

With (14), numerical problems may arise with finite precision arithmetic for small values of ω. These can be circumvented by using the small-ω approximation

$$\Phi_{C_3}(\omega) \approx 1 - \frac{w_3^2 \omega^2}{4}\,, \tag{15}$$

which, in turn, results from the large-x approximation

$$\mathrm{E}_1(x) \approx x^{-1} e^{-x} (1 - x^{-1})\,. \tag{16}$$

As a sanity check, we note that in all cases

$$\lim_{w_n \to 0} \Phi_{C_n}(\omega) = 1\,, \tag{17}$$

as it should for any pdf with all probability mass in the origin, i.e., $w_n = 0$. Therefore, the contribution of $\Phi_{C_n}(\omega)$ in (11) vanishes as w_n approaches zero. In the general n-Rayleigh case given in (10) verification of (17) requires study of the asymptotic behavior of the Meijer G-function; for details we refer to [19].

The corresponding cumulative distribution function (cdf) of (11) is defined as $F_{R_N^\star}(t) = \int_0^t f_{R_N^\star}(r)\,\mathrm{d}r$. Changing the order of integration and noting that [18, §5.56.2]

$$\int_0^t x J_0(ax)\;\mathrm{d}x = \frac{t}{a} J_1(at)\,,$$

we have from (11) the cdf of $R_N^\star$ for arbitrary N as

$$F_{R_N^\star}(t) = \int_0^\infty \omega \prod_{n=0}^{N} \Phi_{C_n}(\omega) J_1(t\omega)\;\mathrm{d}\omega\,. \tag{18}$$

Evaluation of the distribution functions (11) and (18) requires, in general, numerical integration, which is made more difficult by the oscillation of the Bessel function for r or t larger than, say, one. For this reason, using an adaptive integrator routine intended for oscillating integrands is recommended. In numerical experiments we used the Clenshaw-Curtis method, which is implemented in e.g. QUADPACK [31], and was able to compute the integral reliably. Alternatively, numerical Hankel transform [32] or other efficient numerical algorithms may also be used [33].

We remark that while in this paper we focus on the signal model (1) whose nth component has an n-Rayleigh amplitude, the results herein can be extended to more general signal models by simply replacing $\Phi_{C_n}(\omega)$ in (11) with another characteristic function, e.g. that of a product of n Nakagami-m [23] or n generalized gamma variables [34]. These more general characteristic functions can be expressed in terms of H- and G-functions functions using the results and identities in [20], [22], [29], [35]. However, the practical value of such highly generalized and bulky probability distributions is questionable as measurement evidence or physical justification to support their use is currently lacking.

B. *Distribution functions in series form*

Based on the general theory of positive random variables, it is also possible to derive the distribution functions in series forms, that result in computationally simpler implementations that do not require numerical evaluation of the generalized hypergeometric functions. In particular, it is known that the density of a positive random variable can be expressed in a series involving its moments and Laguerre polynomials [21], [27]. With this approach the density of $R_N^\star$ is given by

$$f_{R_N^\star}(r) = 2\beta r e^{-\beta r^2} \sum_{m=0}^{\infty} C_m L_m(\beta r^2)\,, \tag{19}$$

where $L_m(x)$ is the mth order Laguerre polynomial defined in Table I, and

$$C_m = \sum_{k=0}^{m} \frac{(-\beta)^k}{k!} \binom{m}{k} \mu_{R_N^\star}^{(2k)}\,, \tag{20}$$

$$\mu_{R_N^\star}^{(2k)} = \sum_{l=0}^{k} \binom{k}{l}^2 [(k-l)!]^N \mu_{R_{N-1}^\star}^{(2l)} w_N^{2k-2l}\,. \tag{21}$$

The parameter $0 < \beta < \infty$ is a freely selectable constant that tunes the convergence of the series [27]. The even moments of $R_N^\star$ can be computed recursively with initial value $\mu_{R_0^\star}^{(2k)} = w_0^{2k}$. The proof of the recursion formula (21) is given in the appendix.

The corresponding series form of the cdf can be obtained by integrating (19) from 0 to t. Using the definition of the Laguerre polynomial from Table I, a little effort reveals that

$$\int_0^t 2\beta r e^{-\beta r^2} L_m(\beta r^2)\,\mathrm{d}x = \sum_{k=0}^{m} \frac{(-1)^k}{k!} \binom{m}{k} \Gamma_1(k+1, \beta t^2)\,, \tag{22}$$

where $\Gamma_1(a,x)$ is the lower incomplete gamma function. The distribution function for arbitrary N is therefore given by

$$F_{R_N^\star}(t) = \sum_{m=0}^{\infty}\sum_{k=0}^{m} \frac{(-1)^k}{k!}\binom{m}{k} C_m\, \Gamma_1(k+1, \beta t^2)\,, \tag{23}$$

where C_m was given in (20).

IV. Special case: second-order scattering

The Laguerre-type series expansions from the previous section allow computation of numerical values for the amplitude distribution of Nth order scattering. However, optimum selection of the free parameter β is not obvious, and the formulas also involve multi-fold summations. Furthermore, from the general series form it is difficult to see the asymptotic behavior of the distribution near origin, which is of importance when considering fading outage probabilities or high-SNR performance of communications schemes [36]. Therefore it is of interest to seek simpler forms for the distribution functions in special cases. In this section, using a different approach, we derive alternative series expressions for the distribution functions of second-order scattering, of which Rice, Rayleigh and double-Rayleigh distributions are special cases. The second order scattering model results by setting $N=2$ in (1):

$$R_2^\star = \left| w_0 e^{j\theta} + w_1 H_1 + w_2 H_2 H_3 \right| \,.$$

We shall consider the cases $w_0 > 0$ and $w_0 = 0$ separately.

A. The case with line-of-sight component ($w_0 > 0$)

In the appendix it is shown that an alternative series form for $N=2$ is given by

$$\begin{aligned} f_{R_2^\star}(r) &= 2e^{\frac{w_1^2}{w_2^2}} r \sum_{m=0}^{\infty} \frac{(-1)^m w_0^{2m} \Gamma_{\mathrm{u}}\big(-m, \frac{w_1^2}{w_2^2}\big)}{m!\,(w_2^2)^{m+1}} \\ &\quad \times {}_2F_1\left(-m,-m;1;\big(\frac{r}{w_0}\big)^2\right),\ w_1 > 0\,, \end{aligned} \tag{24}$$

where ${}_2F_1(\cdot)$ is the Gauss' hypergeometric function, and $\Gamma_{\mathrm{u}}(-m,x)$ is the upper incomplete gamma function. It can be shown that for $w_2 \to 0$, $f_{R_2^\star}(r)$ reduces to the Rician density function. The upper incomplete gamma function can be computed recursively using [18, §8.356.2]

$$\Gamma_{\mathsf{u}}(n+1,x) = n\,\Gamma_{\mathsf{u}}(n,x) + x^n e^{-x}\,, \tag{25}$$

which is valid also for negative integer values of n. The hypergeometric function in (24) is defined by a finite sum due to negative integer input arguments in ${}_2F_1(\cdot)$. More specifically,

$$ {}_2F_1\left(-m,-m;1;x\right) = \sum_{k=0}^{m} \binom{m}{k}^2 x^k\,. \tag{26}$$

The corresponding distribution function is obtained by integrating (24) from 0 to t, and re-interpreting the resulting sum in terms of hypergeometric functions using the Pochhammer symbol notation [note that $(2)_k = (k+1)!$]. The result is

$$\begin{aligned} F_{R_2^\star}(t) &= e^{\frac{w_1^2}{w_2^2}} t^2 \sum_{m=0}^{\infty} \frac{(-1)^m w_0^{2m} \Gamma_{\mathsf{u}}\big(-m, \frac{w_1^2}{w_2^2}\big)}{m!\,(w_2^2)^{m+1}} \\ &\quad \times {}_2F_1\left(-m,-m;2;\big(\frac{t}{w_0}\big)^2\right)\,,\; w_1>0\,, \end{aligned} \tag{27}$$

where ${}_2F_1(\cdot)$ is given by the finite sum

$$ {}_2F_1\left(-m,-m;2;x\right) = \sum_{k=0}^{m} \binom{m}{k}^2 \frac{x^k}{k+1}\,. \tag{28}$$

B. The case without line-of-sight component ($w_0 = 0$)

This special case ("leaky keyhole") has been derived earlier in [16] using a Bessel function expansion similar to (51). In the following, we show that the desired distribution functions emerge as special cases of the more general results in (24) and (27). This is readily verified, since at the limit $w_0 \to 0$, (26) multiplied by w_0^{2m}, i.e.,

$$ w_0^{2m}\, {}_2F_1\left(-m,-m;1;\big(\frac{r}{w_0}\big)^2\right) = \sum_{k=0}^{m} \binom{m}{k}^2 r^{2k} w_0^{2m-2k}\,, \tag{29}$$

clearly approaches r^{2m}. Therefore, as in [16],

$$ f_{R_2^\star}(r) = 2e^{\frac{w_1^2}{w_2^2}} \sum_{m=0}^{\infty} \frac{(-1)^m}{m!} \frac{\Gamma_{\mathsf{u}}\Big(-m, \frac{w_1^2}{w_2^2}\Big)}{(w_2^2)^{m+1}}\, r^{2m+1}\,,\; w_1>0\,. \tag{30}$$

In the special case $w_2 \to 0$, (30) reduces to the Rayleigh pdf. This can be shown by applying an asymptotic expansion for $\Gamma_{\mathrm{u}}(-m, \frac{w_1^2}{w_2^2})$, and noting that the leftover is a series representation of the exponential function.

The distribution function can be obtained by integrating the series (30) term by term, or by a limit operation similar to (29). The resulting cdf in series form is

$$F_{R_2^\star}(t) = e^{\frac{w_1^2}{w_2^2}} \sum_{m=0}^{\infty} \frac{(-1)^m}{(m+1)!} \frac{\Gamma_{\mathrm{u}}\Big(-m, \frac{w_1^2}{w_2^2}\Big)}{(w_2^2)^{m+1}} \, t^{2m+2} \, , \; w_1 > 0 \, . \tag{31}$$

The series forms and (24), (27), (31) and (30) converge for all finite r and t. However, the speed of convergence depends heavily on r and t; for large values it can be slow. The convergence also depends on the values of the parameters. It can be shown that for large m the convergence of (24) and (27) slows down as the ratio w_0^2/w_1^2, i.e., the Rician K factor, increases (for fixed r or t). Similarly, with (30) and (31) more terms are required for convergence as $w_1 \to 0$. In practice, the series forms are most useful for asymptotic work, such as numerical or analytical evaluation of outage SNR. For $t \ll 1$ or $r \ll 1$, it is enough to take only one or two first terms in the series expansions. Retaining only the first term in (30) and (31) results in the approximations

$$f_{R_2^\star}(r) \approx \frac{2e^{\frac{w_1^2}{w_2^2}} \, \Gamma_{\mathrm{u}}\Big(0, \frac{w_1^2}{w_2^2}\Big)}{w_2^2} \, r \, , \; w_1 > 0 \, , \tag{32}$$

$$F_{R_2^\star}(t) \approx \frac{e^{\frac{w_1^2}{w_2^2}} \, \Gamma_{\mathrm{u}}\Big(0, \frac{w_1^2}{w_2^2}\Big)}{w_2^2} \, t^2 \, , \; w_1 > 0 \, . \tag{33}$$

Here (33) is useful for evaluating outage probabilities, where $t \ll 1$.

An interesting observation can be made from (32). In [36], it has been shown that the the diversity order of a modulation scheme depends only on the behavior of the amplitude density function near origin. For example, the Rayleigh density can be approximated as $f_{R_1}(r) \approx \frac{2r}{w_1^2}$ for $r \ll 1$, which leads to unit diversity order since $f_{R_1}(r)$ can be approximated with a first-degree polynomial [36]. What is surprising here is that also (32) is a first-degree polynomial, which implies that second-order scattering leads to the same diversity order as the Rayleigh channel. Therefore the diversity order seems to be dominated by the lowest order scattering (excluding the LOS component). This clearly has some implications on communication system performance over multiple scattering channels as well as measurement data analysis. We shall give some further remarks on this issue in Section VI.

V. Estimation of mixture weights based on the method of moments

For radio propagation studies the key task is to verify, by means of radio channel measurements, how often and under what conditions multiple scattering appears in nature. To facilitate such studies it is important to derive methods for estimating the mixture weights $\{w_n\}_{n=0}^{N}$ from measurement data. While maximum likelihood estimation would be the optimal estimation method, the complicated form of the probability density function renders this approach impractical. Simple estimators can be obtained by applying the method of moments [37]. The basic idea is to equate sample moments with the theoretical moments to form a group of equations from which the unknown mixture weights can be solved. In what follows, we provide estimation formulas for $N = 2$. The estimators for higher order scattering can be obtained in a similar way.

We shall denote Q independent noiseless samples of $R_2^\star$ with $\{r_q\}_{q=1}^{Q}$. In this section we shall also use the following short-hand notation for the theoretical and sample moments of $R_2^\star$:

$$\mu_{2k} = \mu_{R_2^\star}^{(2k)} \tag{34}$$

$$S_{2k} = \frac{1}{Q}\sum_{q=1}^{Q} r_q^{2k}\,. \tag{35}$$

There should be no confusion with other notation in the paper, since all results in this section apply to the special case $N = 2$.

A. Second-order scattering with LOS component ($w_0 > 0$)

To estimate $\{w_0, w_1, w_2\}$ we need to compute three theoretical moments. It is usually preferable to select low-order moments, as their estimates have smaller variance. From (21), we have for the first three even moments:

$$\mu_2 = w_0^2 + w_1^2 + w_2^2 \,, \tag{36}$$

$$\begin{aligned}\mu_4 &= 4w_2^4 + 4(w_0^2 + w_1^2)w_2^2 \\ &\quad + 2w_1^4 + 4w_0^2 w_1^2 + w_0^4 \,,\end{aligned} \tag{37}$$

$$\begin{aligned}\mu_6 &= 36w_2^6 + 6w_1^6 + w_0^6 + 36w_2^4(w_0^2 + w_1^2) \\ &\quad + 9w_2^2(2w_1^4 + 4w_0^2 w_1^2 + w_0^4) \\ &\quad + 18w_0^2 w_1^4 + 9w_0^4 w_1^2 \,.\end{aligned} \tag{38}$$

Estimates for the squared mixture weights $\{w_n^2\}_{n=0}^2$ can be solved numerically by replacing the theoretical moments $\{\mu_{2k}\}_{k=1}^3$ with the sample moments $\{S_{2k}\}_{k=1}^3$ in (36) – (38), and solving for $\{w_n^2\}_{n=0}^2$. Due to randomness of the sample moments, for finite Q, the system of nonlinear equations may have non-positive solutions; this problem is more evident for small Q. Instead of attempting to solve the system exactly, one may opt for solving the associated non-linear least squares minimization problem, where the solutions are constrained to be non-negative.

B. Second-order scattering without LOS component ($w_0 = 0$)

For the leaky keyhole channel, LOS component mixture weight is zero, and the system of equations can be solved from the second and fourth sample moment. By setting $w_0 = 0$ in (36) and (37), the resulting closed-form estimator appears as

$$\hat{w}_1^2 = S_2 - \hat{w}_2^2 \tag{39}$$

$$\hat{w}_2^2 = \sqrt{\frac{1}{2}S_4 - S_2^2} \,. \tag{40}$$

The estimates are very simple to compute from a given data sample.

For measurement data analysis, it is of practical importance to have an estimate of the mean square error (MSE) of the estimator. In the appendix it is shown that the MSE of $\hat{w}_2^2$ can be upper bounded as

$$\begin{aligned}\epsilon(\hat{w}_2^2) &\triangleq \mathrm{E}\left[(w_2^2 - \hat{w}_2^2)^2\right] \\ &\leq w_2^4 - 2w_2^2\left(\sqrt{\gamma} - \frac{\xi}{8\gamma^{3/2}}\right) + \gamma \,,\end{aligned} \tag{41}$$

where

$$\gamma = \left(\frac{1}{2} - \frac{1}{Q}\right)\mu_4 - \left(1 - \frac{1}{Q}\right)\mu_2^2\,, \tag{42}$$

$$\xi = a - b + c - \gamma^2\,, \tag{43}$$

and

$$a = \frac{1}{4Q}\left[\mu_8 + (Q-1)\,\mu_4^2\right]\,, \tag{44}$$

$$b = \frac{1}{Q^2}\Big\{\mu_8 + (Q-1)\mu_4^2 + (Q-1)\mu_2\big[2\mu_6 + (Q-2)\mu_4\mu_2\big]\Big\}\,, \tag{45}$$

$$c = \frac{1}{Q^3}\Big[\mu_8 + 4(Q-1)\mu_6\mu_2 + 3(Q-1)\mu_4^2 + 6(Q-1)(Q-2)\mu_4\mu_2^2 + (Q-1)(Q-2)(Q-3)\mu_2^4\Big]\,. \tag{46}$$

The even moments of $R_2^\star$ can be computed using (21). The upper bound is quite tight for large Q, as will be illustrated in the next section. A bound for the mean square error of $\hat{w}_1^2$ can be derived in a similar way. However, from numerical experiments it is found that the MSE of $\hat{w}_1^2$ is roughly the same as that of $\hat{w}_2^2$, and therefore to save paper we omit the result.

Taking expectation of (40) and applying Jensen's inequality it is clear that, for finite Q, (40) underestimates w_2^2. Consequently w_1^2 will be overestimated. However, as with most moment-based estimators, $\hat{w}_1^2$ and $\hat{w}_2^2$ are asymptotically unbiased, i.e., the bias diminishes as the number of samples increases [37]. This is also evident from (42), from which

$$\lim_{Q\to\infty} \mu_X = w_2^4\,,$$

and hence

$$w_2^2 - \lim_{Q\to\infty} \mathrm{E}[\hat{w}_2^2] = 0$$

indicating that $\hat{w}_2^2$ is a consistent estimator of w_2^2. It then follows that $\hat{w}_1^2$ is also a consistent estimator.

VI. Numerical examples

In all numerical examples that follow the mixture weights are normalized so that $E[(R_N^\star)^2] = \sum_{n=0}^{N} w_n^2 = 1$. For example, $w_n^2 = 1$ then implies that mixture weights other than n are zero, i.e., $R_N^\star = R_n$ has the n-Rayleigh distribution.

A. Pdfs and cdfs of $R_N^\star$

In Figs. 3–4 we plot the distribution functions for a few values of $\{w_n^2\}$. In Fig. 3 n-Rayleigh densities (i.e., $w_n^2 = 1$) are shown for $n = 1, \ldots, 5$. We also show two examples of third-order scattering: $w_0^2 = 0.909$, $w_1^2 = w_2^2 = w_2^3 = (1 - w_0^2)/3$, and $w_0^2 = 0$, $w_1^2 = w_2^2 = 0.1$, $w_3^2 = 0.8$.

The figures confirm the well-known fact that multiple scattering widens the tails of the amplitude distribution compared to single scattering (Rayleigh) amplitude pdf [3]. Therefore, the fading is more severe because of the multiple scattering radio propagation environment, and consequently communication will require higher average SNR to achieve the same error performance than over a Rayleigh channel. The thick tails may also complicate radio channel measurements. Special attention should be placed on the linear dynamic range of the measurement equipment so that the measured amplitude is not distorted by the measurement system. For example, with the double-Rayleigh distribution the amplitude range between 0.5% and 99.5% percentiles has dynamic range of 42 decibels, which is considerably larger than the corresponding value of 30 dB for Rayleigh distributed amplitude. By dynamic range we mean here the ratio $\frac{t_{max}}{t_{min}}$, where $F_{R_2}(t_{min}) = 0.005$ and $F_{R_2}(t_{max}) = 0.995$.

Fig. 4 is a Rayleigh probability graph where the Rayleigh distribution shows as a straight line, whereas other distribution functions appear curved. From the cdfs in Fig. 4 we note that the decay rates of the n-Rayleigh distributions for $n > 1$ near origin are slightly slower than that of the Rayleigh cdf. This implies that diversity order (high-SNR slope of error probability curve [36]) of the pure n-Rayleigh channel is less than one, i.e., worse than the Rayleigh diversity order. The slopes of third order scattering with nonzero w_1, on the other hand, show the same decay rate as the conventional Rayleigh cdf. This could be one reason why multiple scattering is difficult to detect in channel measurements, since it is unlikely that in real-world radio propagation channels

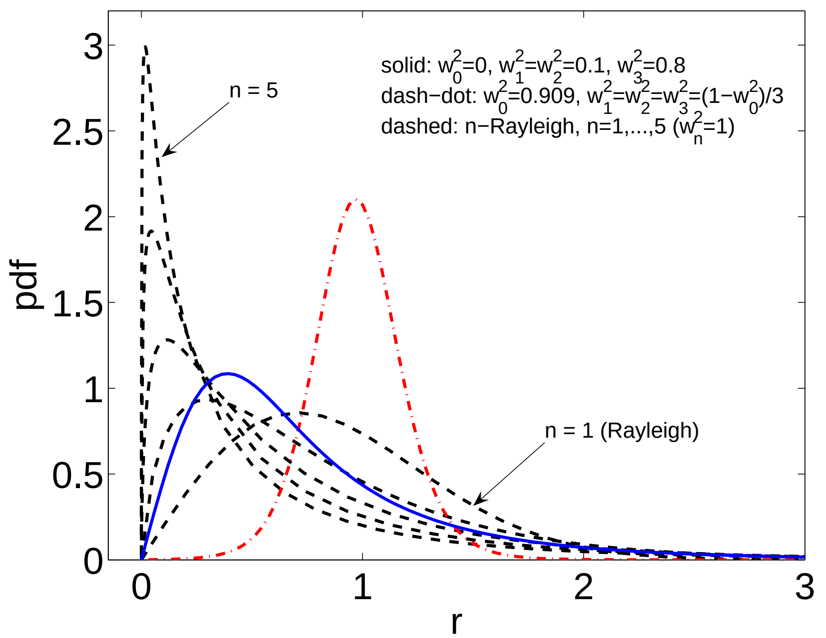

Fig. 3. Probability densities of $R_N^\star$ plotted for varying $\{w_n^2\}$. In all cases $\sum_{n=0}^{N} w_n^2 = 1$.

the single scattering component would be exactly zero[2]. Of course, a horizontal shift can still be seen in the cdf. From communication system point of view, this would mean that the diversity order of a multiple scattering channel with $w_1 > 0$ would be the same as that of the Rayleigh channel. Detailed examination of these issues, however, is a topic for further study.

B. Moment-based estimation of parameters

We consider the case of second-order scattering with $w_0 = 0$. In Fig. 5 we plot the MSE of $\hat{w}_1^2$ and $\hat{w}_2^2$ obtained using (39) and (40). The results have been estimated from a Monte Carlo simulation with 10^5 trials for each value of Q. For small Q it sometimes happens that $\hat{w}_2^2$ from (40) is negative. In this case we set $\hat{w}_2^2 = 0$. From Fig. 5 we note that the MSE is larger for w_2^2. Also, MSE decreases inversely proportional to the number of samples as predicted by the general theory of moment-based estimation. We also plot the upper bound (41) on MSE of $\hat{w}_2^2$. It can be seen that the bound is tight for $Q > 100$ and can hence be used in evaluation of the number of samples required for reliable estimation of the mixture weights. Based on Fig.

[2]In practical measurement, Gaussian measurement noise is added to the measured impulse response hence always resulting in positive w_1.

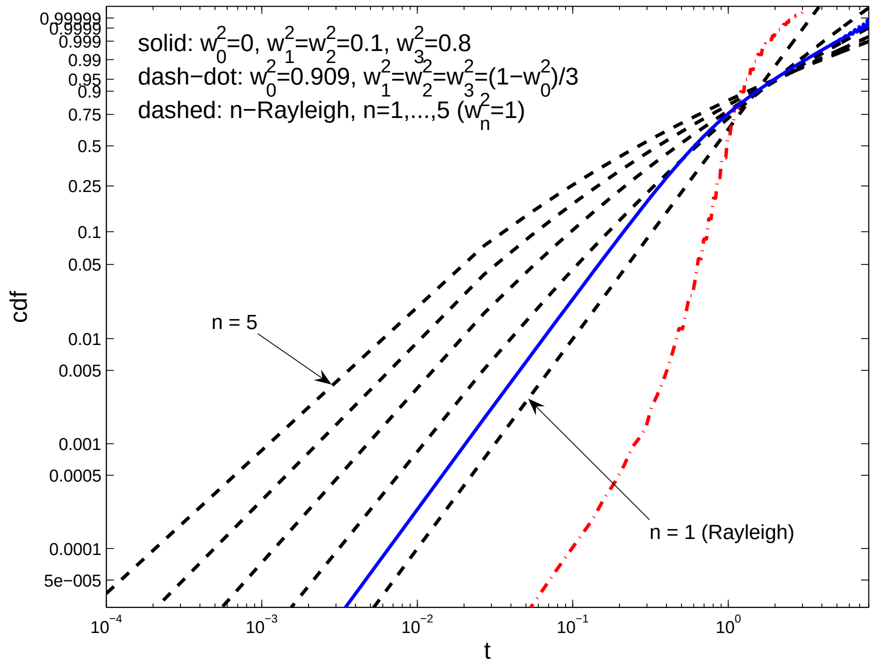

Fig. 4. Cumulative distribution functions of $R_N^\star$ plotted in a Rayleigh probability plot for varying $\{w_n^2\}$.

5 we can say that, with the present estimator, about a thousand or more stationary samples are required for reliable estimation of the mixture weights from measurement data.

VII. Conclusion

We have derived the distribution functions (pdf and cdf) of amplitude of multiple scattering radio channel in integral and series forms. The special case of second-order scattering was discussed in detail. We also derived a computationally simple estimator for the mixture weights of a second-order scattering process. The most interesting open problems and future work are related to the verification of the environmental conditions under which the multiple scattering radio propagation occurs in nature. This is likely to require carefully planned radio channel measurements and meticulous measurement data analysis. Another topic for future work is the evaluation of the impact of multiple scattering on communication system performance. The results presented in this paper serve as necessary groundwork to facilitate these studies.

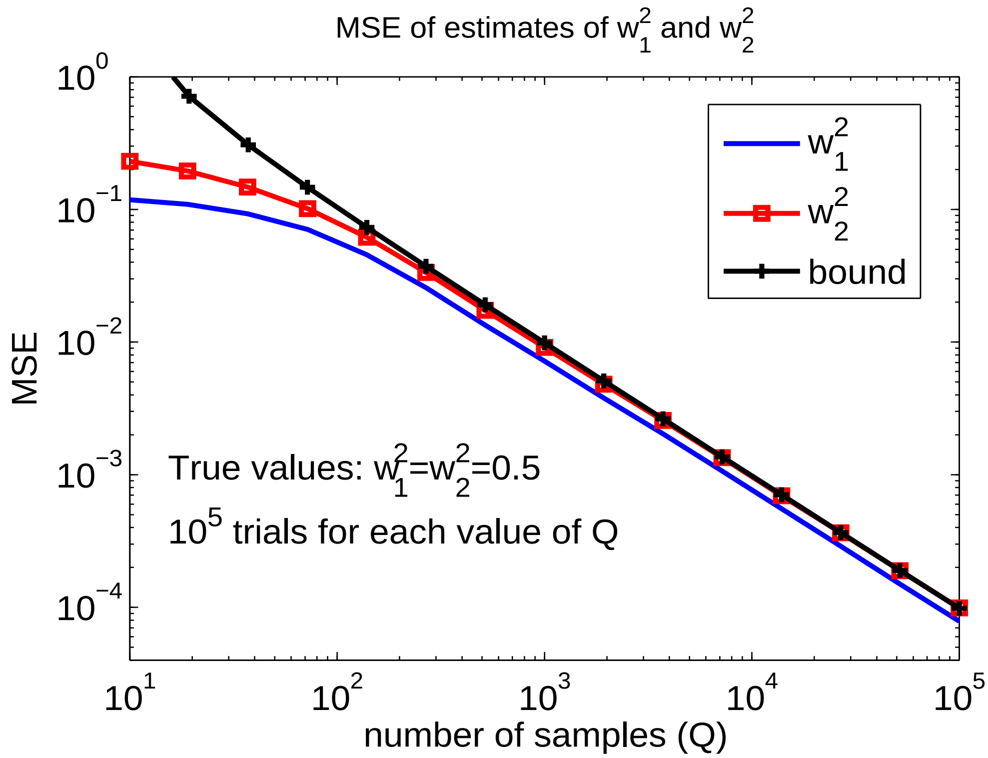

Fig. 5. Mean square error of $\hat{w}_1^2$ and $\hat{w}_2^2$. True values are $w_1^2 = w_2^2 = 0.5$, $w_0^2 = 0$. Estimates are computed with (39) and (40). The upper bound (41) is also shown.

APPENDIX I
MISCELLANEOUS PROOFS

In this appendix we sketch some of the intermediate steps missing in the main text.

A. Eq. (21)

Applying a general recursion formula for the modulus of a sum of independent circularly symmetric random variables [38] we obtain

$$\mu_{R_N^\star}^{(2k)} = \sum_{m=0}^{k} \binom{k}{m}^2 \mu_{R_{N-1}^\star}^{(2m)} \mu_{R_N}^{(2k-2m)} \,. \tag{47}$$

Moments of an n-Rayleigh random variable are [17]

$$\mu_{R_n}^{(h)} = w_n^h \left[\Gamma\left(\frac{h}{2}+1\right)\right]^n \,. \tag{48}$$

From (48), the even moments of R_n read as

$$\mu_{R_n}^{(2k)} = w_n^{2k}(k!)^n\,, \quad k = 0, 1, 2, \dots\ . \tag{49}$$

Hence, plugging (49) to (47), we arrive at (21).

B. Eq. (30)

Inserting (8), (12) and (13) into (11) we have to evaluate

$$f_{R_2^\star}(r) = r\int_0^\infty \frac{4\omega}{4 + w_2^2\omega^2}\, e^{-\frac{w_1^2\omega^2}{4}} J_0(w_0\omega)J_0(r\omega)\ \mathrm{d}\omega\,. \tag{50}$$

Using the identity [18, §8.442.2]

$$\begin{aligned} J_0(w_0\omega)J_0(r\omega) &= \sum_{m=0}^\infty \frac{(-1)^m(w_0\omega)^{2m}}{2^{2m}(m!)^2} \\ &\quad \times {}_2F_1\left(-m, -m; 1; (\frac{r}{w_0})^2\right), \end{aligned} \tag{51}$$

with ${}_2F_1(a, b; c; x)$ denoting the Gauss' hypergeometric function, we can write (50) as

$$\begin{aligned} f_{R_2^\star}(r) &= r\sum_{m=0}^\infty \frac{(-1)^m w_0^{2m}}{2^{2m}(m!)^2}\, {}_2F_1\left(-m, -m; 1; (\frac{r}{w_0})^2\right) \\ &\quad \times \underbrace{\int_0^\infty \frac{\omega^{2m+1}}{1 + b\omega^2} e^{-a\omega^2}\ \mathrm{d}\omega}_{I_m}\ . \end{aligned} \tag{52}$$

where $a = \frac{w_1^2}{4}, b = \frac{w_2^2}{4}$ for brevity. The integral I_m, which appears as a coefficient in the series, can be evaluated by substituting $y = 1 + b\omega^2$, resulting in

$$I_m = \frac{e^{\frac{a}{b}}}{2b^{m+1}} \int_1^\infty \frac{(y-1)^m}{y}\, e^{-\frac{a}{b}y}\ \mathrm{d}y\,. \tag{53}$$

This is a standard integral [18, §3.383.9] given by

$$I_m = \frac{e^{\frac{a}{b}}}{2b^{m+1}}\, \Gamma(m+1)\Gamma_{\mathrm{u}}\Big(-m, \frac{a}{b}\Big), \quad a > 0\,, \tag{54}$$

where $\Gamma_{\mathrm{u}}(n, x)$ is the upper incomplete gamma function, which is defined also when n is a negative integer, unlike the gamma function $\Gamma(n)$, which is singular at these points. After some simplifications, we arrive at the desired result.

C. Eq. (41)

We denote for brevity

$$X = \frac{1}{2}S_4 - S_2^2\,, \tag{55}$$

and its mean and variance with $\mu_X = \mathrm{E}[X]$ and $\mathrm{var}[X]$, respectively. Note that $X = \hat{w}_2^4$. The MSE of $\hat{w}_2^2$ is given by

$$\begin{aligned} \epsilon(\hat{w}_2^2) &\triangleq \mathrm{E}\left[(w_2^2 - \hat{w}_2^2)^2\right] \\ &= w_2^4 - 2w_2^2\,\mathrm{E}[\hat{w}_2^2] + \mathrm{E}[\hat{w}_2^4] \\ &= w_2^4 - 2w_2^2\,\mathrm{E}\left[\sqrt{X}\right] + \mu_X \end{aligned} \tag{56}$$

Expanding $\sqrt{X}$ in a Taylor series about μ_X and taking expectation we arrive at the lower bound

$$\mathrm{E}\left[\sqrt{X}\right] \geq \sqrt{\mu_X} - \frac{\mathrm{var}[X]}{8\mu_X^{3/2}}\,, \tag{57}$$

where we truncated the series after the third term. Using (57) we can upper bound (56) as

$$\epsilon(\hat{w}_2^2) \leq w_2^4 - 2w_2^2\left(\sqrt{\mu_X} - \frac{\mathrm{var}[X]}{8\mu_X^{3/2}}\right) + \mu_X\,. \tag{58}$$

Formulas for μ_X and $\mathrm{var}[X]$ are needed for computing the bound (41). The mean value of X can be shown to be

$$\mu_X = \left(\frac{1}{2} - \frac{1}{Q}\right)\mu_4 - \left(1 - \frac{1}{Q}\right)\mu_2^2\,. \tag{59}$$

To compute $\mathrm{var}[X]$, it suffices to find $\mathrm{E}[X^2]$, since $\mathrm{var}[X] = \mathrm{E}[X^2] - \mu_X^2$. This is in principle straightforward, but quite tedious. Omitting details, the end result is

$$\mathrm{E}[X^2] = a - b + c\,, \tag{60}$$

where a,b, and c are given in (44)–(46). Denoting $\gamma = \mu_X$ and $\xi = \mathrm{E}[X^2] - \mu_X^2$, the desired result follows.

ACKNOWLEDGMENT

We thank Jussi Salmi for helping with the numerical verification of (30), and Jan Eriksson for his observation regarding the Laplacianity of (13).

REFERENCES

[1] W. C. Jakes, Ed., *Microwave Mobile Communications*. IEEE Press, 1994.

[2] G. C. Hess, *Handbook of Land-Mobile Radio System Coverage*. Artech House, Inc, 1997.

[3] J. B. Andersen and I. Z. Kovács, "Power distributions revisited," in *Proc. COST273 3rd Management Committee Meeting*, Jan. 17-18, 2002, Guildford, UK, TD(02)004.

[4] J. B. Andersen, "Statistical distributions in mobile communications using multiple scattering," in *Proc. 27th URSI General Assembly*, Maastricht, Netherlands, Aug. 2002.

[5] B. A. Dolan, "The Mellin transform for moment-generation and for the probability density of products and quotients of random variables," *Proc. IEEE*, vol. 52, no. 12, pp. 1745 – 1746, Dec. 1964.

[6] D. Chizhik, G. J. Foschini, and R. A. Valenzuela, "Capacities of multi-element transmit and receive antennas: Correlations and keyholes," *El. Lett.*, vol. 36, no. 13, pp. 1099 –1100, Jun. 2000.

[7] D. Gesbert, H. Bölcskei, D. A. Gore, and A. J. Paulraj, "Outdoor MIMO wireless channels: Models and performance prediction," *IEEE Trans. Commun.*, vol. 50, no. 12, pp. 1926–1934, Dec. 2002.

[8] M. O. Hasna and M.-S. Alouini, "A performance study of dual-hop transmissions with fixed gain relays," *IEEE Trans. Wireless Commun.*, vol. 3, no. 6, pp. 1963–1968, Nov. 2004.

[9] J. N. Laneman, D. N. C. Tse, and G. W. Wornell, "Cooperative diversity in wireless networks: Efficient protocols and outage behavior," *IEEE Trans. Inform. Theory*, vol. 50, no. 12, pp. 3062–3080, Dec. 2004.

[10] C. S. Patel, G. L. Stüber, and T. G. Pratt, "Statistical properties of amplify and forward relay fading channels," *IEEE Trans. Veh. Technol.*, vol. 55, no. 1, pp. 1–9, Jan. 2006.

[11] V. Erceg, S. J. Fortune, J. Ling, A. Rustako, and R. A. Valenzuela, "Comparisons of a computer-based propagation prediction tool with experimental data collected in urban microcellular environments," *IEEE J. Select. Areas Commun.*, vol. 15, no. 4, pp. 677–684, May 1997.

[12] P. Almers, F. Tufvesson, and A. F. Molisch, "Measurement of keyhole effect in a wireless multiple-input multiple-output (MIMO) channel," *IEEE Commun. Lett.*, vol. 7, no. 8, pp. 373–375, Aug. 2003.

[13] ——, "Keyhole effects in MIMO wireless channels - measurements and theory," in *Proc. Globecom'03*, vol. 4, Dec. 2003, pp. 1781–1785.

[14] I. Z. Kovács, "Radio channel characterization for private mobile radio systems," Ph.D. dissertation, Aalborg University, Center for PersonKommunikation, 2002.

[15] I. Z. Kovács, P. Eggers, K. Olesen, and L. Petersen, "Investigations of outdoor-to-indoor mobile-to-mobile radio communication channels," in *Proc. IEEE 56th Vehicular Technology Conference (VTC-Fall)*, vol. 1, Sept. 2002, pp. 430–434.

[16] J. Salo, J. Salmi, and P. Vainikainen, "Distribution of the amplitude of a sum of singly and doubly scattered fading radio signal," in *Proc. IEEE Veh. Tech. Conf. (VTC-Spring)*, Stockholm, Sweden, May 30 - June 1 2005.

[17] J. Salo, H. M. El-Sallabi, and P. Vainikainen, "The distribution of the product of independent Rayleigh random variables," *IEEE Trans. Antennas Propagat.*, vol. 54, no. 2, pp. 639–643, Feb. 2006.

[18] I. Gradshteyn and I. Ryzhik, *Table of integrals, series, and products*, 4th ed. Academic Press, Inc., 1980.

[19] Y. L. Luke, *Special functions and their approximations*, ser. Mathematics in Science and Engineering. Academic Press, 1969, vol. 1.

[20] “The Wolfram Functions Site,” http://functions.wolfram.com/.

[21] M. Nakagami, “The m-distribution - a general formula of intensity distribution of rapid fading,” in *Statistical Methods in Radio Wave Propagation*, W. C. Hoffman, Ed. Pergamon Press, 1960, pp. 3–36.

[22] A. M. Mathai, “Products and ratios of generalized gamma variates,” *Skandinavisk Aktuarietidskrift*, pp. 193–198, 1972.

[23] G. K. Karagiannidis, N. C. Sagias, and T. Mathiopoulos, “The N*Nakagami fading channel model,” in *Proc. Int. Symp. Wireless Comm. Syst.*, Sept. 2005, pp. 185–189.

[24] N. C. Sagias, P. T. Mathiopoulos, P. S. Bithas, and G. K. Karagiannidis, “On the distribution of the sum of generalized gamma variates and applications to satellite digital communications,” in *Proc. Int. Symp. Wireless Comm. Syst.*, Sept. 2005, pp. 785–789.

[25] R. Bracewell, *The Fourier Transform and Its Applications*. McGraw-Hill, Inc., 1965.

[26] K.-T. Fang, S. Kotz, and K. W. Ng, *Symmetric multivariate and related distributions*, ser. Monographs on statistics and applied probability. New York, USA: Chapman and Hall, 1990.

[27] A. Abdi, H. Hashemi, and S. Nader-Esfahani, “On the pdf of the sum of random vectors,” *IEEE Trans. Commun.*, vol. 48, no. 1, pp. 7–12, Jan. 2000.

[28] G. D. Durgin, *Space-Time Wireless Channels*. Prentice-Hall, 2003.

[29] A. M. Mathai and R. K. Saxena, *Generalized Hypergeometric Functions with Applications in Statistics and Physical Sciences*, ser. Lecture notes in mathematics. Springer-Verlag, 1973.

[30] A. M. Mathai, *A Handbook of Generalized Special Functions for Statistical and Physical Sciences*. Oxford, UK: Clarendon Press, 1993.

[31] R. Piessens, E. de Doncker-Kapenga, C. Überhuber, and D. Kahaner, *QUADPACK, A Subroutine Package for Automatic Integration*. Springer-Verlag, 1983.

[32] J. Markham and J.-A. Conchello, “Numerical evaluation of Hankel transforms for oscillating functions,” *J. Opt. Soc. Am. A*, vol. 20, no. 4, pp. 621–630, Apr. 2003.

[33] S. K. Lucas, “Evaluating infinite integrals involving products of Bessel functions,” *Journal of Computational and Applied Mathematics*, vol. 64, pp. 269–282, 1995.

[34] A. J. Coulson, A. G. Williamson, and R. G. Vaughan, “Improved fading distribution for mobile radio,” *IEE Proc. Comm.*, vol. 145, no. 3, pp. 197–202, June 1998.

[35] B. D. Carter and M. D. Springer, “The distribution of products, quotients and powers of independent H-Function variates,” *SIAM Journal on Applied Mathematics*, vol. 33, no. 4, pp. 542–558, 1977.

[36] Z. Wang and G. B. Giannakis, “A simple and general parameterization quantifying performance in fading channels,” *IEEE Trans. Commun.*, vol. 51, no. 8, pp. 1389–1398, Aug. 2003.

[37] S. M. Kay, *Fundamentals of Statistical Signal Processing: Estimation Theory*. Prentice-Hall International, 1993.

[38] J. Goldman, “Moments of the sum of circularly symmetric random variables,” *IEEE Trans. Inform. Theory*, vol. 18, no. 2, pp. 297–298, Mar. 1972.